NIH Public Access
Author Manuscript
J Neurosci Methods. Author manuscript; available in PMC 2012 January 30.

Published in final edited form as:
J Neurosci Methods. 2011 January 30; 195(1): 24–29. doi:10.1016/j.jneumeth.2010.11.008.

Calcium Imaging of Auditory Nerve Fiber Terminals in the Cochlear Nucleus

Soham Chanda, **Sangrok Oh**, and **Matthew A. Xu-Friedman***
Department of Biological Sciences, 109 Cooke Hall, University at Buffalo, State University of New York, Buffalo, NY 14260, USA

Abstract

One important model for understanding neuronal computation is how auditory information is transformed at the synapses made by auditory nerve (AN) fibers on the bushy cells (BCs) in the anteroventral cochlear nucleus (AVCN). This transformation is influenced by synaptic plasticity, the mechanisms of which have been studied primarily using postsynaptic electrophysiology. However, it is also important to make direct measurements of the presynaptic terminal to consider presynaptic mechanisms. Here we introduce a technique for doing that using calcium imaging of presynaptic AN terminals, by injecting dextran-conjugated fluorophores into the cochlea. To measure the calcium transients, we used calcium-sensitive fluorophores, and measured the changes in fluorescence upon stimulation. As an example of the application of this technique, we showed that activation of $GABA_B$ receptors reduces presynaptic calcium influx. This technique could be further extended to study the effects of activity- and other neuromodulator-dependent plasticities on AN terminals.

Keywords

endbulb; calcium imaging; auditory nerve; bushy cell

Introduction

The auditory nerve (AN) has served as an important model system for understanding the processing of information in the nervous system. The synapses formed by AN fibers onto bushy cells (BCs) in the anteroventral cochlear nucleus (AVCN) are called endbulbs of Held. Endbulbs show remarkable adaptations for relaying the temporal information of auditory signals (Brawer and Morest, 1975; Lorente de Nó, 1981; Ryugo and Fekete, 1982; Fekete et al., 1984; Oertel, 1991; Ostapoff and Morest, 1991; Ryugo et al., 1991; Ryugo and Sento, 1991) from AN to higher centers involved in sound localization (Cant and Casseday, 1986; Spirou et al., 1990; Smith et al., 1991; Smith et al., 1993).

The endbulb is particularly interesting because both pre- and postsynaptic activity have been well-studied *in vivo*, so the transformation of sensory information that takes place at this synapse has been addressed. This transformation may be influenced by various forms of

© 2010 Elsevier B.V. All rights reserved.

*Address for correspondence: Matthew A. Xu-Friedman, 109 Cooke Hall, Buffalo, NY 14260, Phone: [716] 645-2363, Fax: [716] 645-2975, mx@buffalo.edu .

Publisher's Disclaimer: This is a PDF file of an unedited manuscript that has been accepted for publication. As a service to our customers we are providing this early version of the manuscript. The manuscript will undergo copyediting, typesetting, and review of the resulting proof before it is published in its final citable form. Please note that during the production process errors may be discovered which could affect the content, and all legal disclaimers that apply to the journal pertain.

NIH-PA Author Manuscript
NIH-PA Author Manuscript
NIH-PA Author Manuscript

NIH-PA Author Manuscript

NIH-PA Author Manuscript

NIH-PA Author Manuscript

activity- or neuromodulator-dependent synaptic plasticity. Plasticity has been the subject of considerable study at the endbulb, but so far this has been limited to postsynaptic electrophysiology (Bellingham et al., 1998; Gardner et al., 1999; Wang and Manis, 2008; Yang and Xu-Friedman, 2008; Chanda and Xu-Friedman, 2010b). In an effort to expand this study to the presynaptic terminal, we describe an approach for studying endbulbs using calcium imaging.

The invention of calcium-sensitive dyes was an important advance for measuring calcium levels and influx (Grynkiewicz et al., 1985), and has now become a standard physiological approach. Calcium imaging has allowed important discoveries about the relationship between neurotransmitter release and calcium influx through presynaptic voltage-gated calcium channels, and the dependence of these on activity and neuromodulation (Zucker and Regehr, 2002). This approach has been most successful at synapses that are particularly well-organized anatomically so that specific types of synapses may be loaded with dyes and studied in isolation.

Typical loading approaches are complicated at the endbulb. One could patch the auditory nerve fiber, and include calcium-sensitive dyes in the patch pipette. However, the somata of AN fibers are located far from the terminals in the spiral ganglion, which is outside the cranium and is typically not preserved in slice preparations. Furthermore, it is difficult to patch endbulbs directly, because they are small and highly fenestrated. Another approach might be to apply acetoxymethylester (AM) forms of dyes into the auditory nerve root, which has been very successful in other preparations (Tsien, 1981; Regehr and Tank, 1991). However, uptake of these by auditory nerve fibers is poor, probably because they are effectively shielded by heavy myelination. Bath application of AM dyes leads to considerable non-specific labeling, so fluorescent signals originate from many non-specific structures. Thus, a different approach for labeling AN fibers specifically would be preferable.

One approach for this is to load dyes in the cochlea. This approach has been used to label AN fibers with neurobiotin by injecting it through the oval window (Limb and Ryugo, 2000). This has also been done with a crystal of diI deposited through a hole in the wall of the cochlea (Maruyama and Ohmori, 2006). We adapted these approaches, and used dextran-conjugated fluorescent dyes for labeling. Here we illustrate the use of this method for anatomical study, as well as to investigate mechanisms of neuromodulator-dependent synaptic plasticity. These are the first measurements of presynaptic calcium influx at the endbulb.

Materials and Methods

All procedures were approved the University at Buffalo’s Institutional Animal Care and Use Committee.

Surgical approach

Loading was done in CBA/CaJ mice (Jackson Laboratories, Bar Harbor, ME) aged postnatal day 16 (P16) to P21. Mice were anesthetized with a dose of 200 mg/kg ketamine: 10 mg/kg xylazine. When the mice were areflexic to paw pinch, they were laid on a warming pad maintained at 37°C (Gaymar Industries INC., Orchard Park, NY) to maintain their body temperature. Puralube Vet Ointment (Pharmaderm, Melville, NY) was applied to protect the eyes. Hair was removed from a small patch of skin posterior to the ear with Nair (Fig. 1A), and the skin was sterilized with 70% ethanol and betadine (Purdue products, Stamford, CT). A small amount of 0.5% marcaine (Hospira Inc, Lake Forest, IL) was applied to the skin.

NIH-PA Author Manuscript

NIH-PA Author Manuscript

NIH-PA Author Manuscript

Next, we made a small cut on the skin posterior to the pinna with scissors, and then detached muscle tissue from the auditory canal by pulling with forceps (Fig. 1B). An incision was made in the auditory canal, and part of the free cartilage was removed (Fig. 1C). The tympanic membrane was disrupted and the malleus was removed (Fig. 1D). This hole was widened by removing part of the bulla on the posterior side to expose the round window (Fig. 1E). The round window was ruptured with a fine insect pin, typically leading to release of clear perilymph. A small hole was drilled just above the line that divides the two turns of the cochlea (Fig. 1E, asterisk) using a fine insect pin. At the ages used here, the wall of the upper turn is particularly soft, but gets somewhat harder after P20.

For dye injection, micropipettes were pulled from borosilicate capillary tubes (Sutter Instruments, Novato, CA) using a P-97 micropipette puller (Sutter Instruments, Novato, CA) with a diameter of about 20 μm. The micropipette was attached to the end of a 1 mm syringe. The syringe was attached to a micromanipulator (Narashige, Japan). The tip of the micropipette was loaded with 1 μl of 20% dextran-conjugated fluorescent dye. This consisted of 20% fluorescein (Fig. 2A) or Texas red (Fig. 2B) conjugated to 3000-MW-dextran, or 10% of the Texas red-dextran plus 10% calcium green-1 or Oregon green 1 conjugated to 3000 or 10,000 MW dextran (Invitrogen) (Fig. 4). The pipette was lowered into the hole made in the wall of the cochlea and the dye was injected into the cochlea by applying light pressure on the plunger (Fig. 1F). After the dye was loaded, the wound was closed using Vetbond (3M, St Paul, MN) and the mouse was injected with 5 mg/kg rimadyl. Mice typically woke 1–2 hr after surgery. After a survival time of 12 hr, mice were sacrificed for brain slicing or anatomy.

Electrophysiology and calcium imaging

Slices in the cochlear nucleus were prepared as described previously (Chanda and Xu-Friedman, 2010b). Briefly, sagittal sections (160 μm thickness) of the cochlear nucleus were prepared in ice-cold solution containing the following (in mM): 76 NaCl, 75 sucrose, 25 $NaHCO_3$, 25 glucose, 2.5 KCl, 1.25 NaH_2PO_4, 7 $MgCl_2$, 0.5 $CaCl_2$. Slices were used for patch-clamping or calcium-imaging using standard recording solution containing the following (in mM): 125 NaCl, 26 $NaHCO_3$, 20 glucose, 2.5 KCl, 1.25 NaH_2PO_4, 1 $MgCl_2$, 1.5 $CaCl_2$, 4 Na L-lactate, 2 Na-pyruvate, 0.4 Na L-ascorbate, bubbled with 95% O_2 and 5% CO_2. All recordings were made at ~34°C in the presence of 10 μM strychnine. The pharmacological agents used were baclofen (100 μM, Sigma, St. Louis, MO) and CGP55845 (2 μM, Tocris Bioscience, Ellisville, MO).

Electrophysiology

For electrophysiology controls, BCs were patched under an Olympus BX51WI microscope with a Multiclamp 700B (Molecular Devices) controlled by ITC-18 (Instrutech) interface driven by custom-written software (mafPC) running in Igor (Wavemetrics). Pipettes were 1–2 MΩ, filled with the following (in mM): 35 CsF, 100 CsC1, 10 EGTA, 10 HEPES. The holding potential for voltage clamp was −70 mV with access resistance 3–7 MΩ, compensated to 70%. AN fibers were stimulated using a glass micropipette placed 30–50 μm away from the cell being recorded with currents of 6–14 μA through a stimulus isolator (WPI A360).

Calcium-imaging

For calcium-imaging, labeled fibers were imaged using a 60X water-immersion objective under a 150 W xenon lightsource (Optiquip Model 770), with excitation/dichroic/emission filters of 560DF55/595/645DF75 (for Texas red) or 480DF40/505/535DF50 (for calcium green and Oregon green). Fluorescence was detected using a Sensicam QE (Cooke Corp.)

NIH-PA Author Manuscript

NIH-PA Author Manuscript

NIH-PA Author Manuscript

controlled by SIDX drivers (Bruxton Corp., Seattle, WA) running in Igor. Results were filtered with a 7-pixel Gaussian.

Immunohistochemistry

After the diffusion step, mice were re-anesthetized, and perfused transcardially with 0.9% NaCl, followed by 4% paraformaldehyde in 0.1 M phosphate buffer. The brains were post-fixed for 2 hour before cryoprotecting overnight in 20% sucrose. Coronal or sagittal sections were made at 40 μm on a sliding microtome (American Optical, Buffalo, NY).

Sections containing the AVCN were collected and washed in 3 5-minute cycles in 0.2 M phosphate buffer saline (PBS), pH~7.6. The sections were then blocked in 0.2 M PBS with 0.1% Triton X-100 (Sigma) and 5% goat serum for two hours. The sections were incubated overnight at 4°C in primary antibody solution containing: anti-CB1 (gift from Mackie lab, Indiana University, Bloomington, IN) at 1:500 concentration, 5% goat serum, and 0.2 M PBS with Triton X-100. The sections were then washed 3 times in 0.2 M PBS solution, and incubated for 2 hours with either Texas-red-conjugated goat anti-rabbit or FITC-conjugated goat anti-rabbit secondary antibody solution (Jackson Immuno Research Laboratories, West Grove, PA) at 1:200 dilution in 0.2 M PBS, 0.1% Triton X-100 and 5% goat serum. The sections were stained with DAPI for cell body labeling, washed in PBS and then mounted on glass slides using Fluoromount G (Southern Biotech). The image in Fig. 2 was acquired using a Zeiss AxioImager Fluorescence Microscope.

Data analysis

Average data are presented as mean ± standard error (SE). Statistical significance was determined using the paired, two-tailed, student's *t*-test.

Results

AN labeling

After injecting dextran-conjugated fluorescein into the cochlea, the AN was strongly labeled (green, Fig. 2A). In a sagittal section of the cochlear nucleus on the ipsilateral side of dye injection, bright labeling was observed in the nerve root (VIII, Fig. 2A) as well as in the dorsal and posterior projection into the AVCN and DCN. In this preparation, two distinct frequency bands were labeled which terminated in different regions of the AVCN. The high frequency band ("*") showed a bifurcation to the AVCN and a collateral heading towards the DCN.

We also prepared examined labeling using coronal sections (Fig. 2B). AN fibers were brightly labeled in the AVCN and in their projections towards DCN (Fig, 2Bi). In the AVCN, we saw labeled AN terminals, which had the characteristic appearance of endbulbs of Held around the postsynaptic cell body (Fig, 2Bii). By contrast, AN fibers in the deep layers of the DCN showed punctate labeling, which are presumably synaptic terminals (Fig, 2Biii). These patterns of labeling were quite consistent from one preparation to the next.

Electrophysiology of labeled endbulbs

There are effects of deafening on the auditory nerve and cochlear nucleus (Salvi et al., 1983; Tucci and Rubel, 1985; Saada et al., 1996; Oleskevich and Walmsley, 2002; Heinz and Young, 2004), and we wanted to know if our surgical procedure affects the physiological properties of the endbulb. To test that, we performed voltage-clamp recordings from postsynaptic BCs while stimulating a presynaptic AN input with trains of pulses (Fig. 3). Endbulb EPSCs showed considerable depression when stimulated at 200 Hz for a BC contralateral to the dye-injected cochlea (Fig. 3A, left trace). Similar depression was

NIH-PA Author Manuscript

NIH-PA Author Manuscript

NIH-PA Author Manuscript

observed from an ipsilateral BC (Fig. 3A, right trace). The kinetics of individual EPSCs did not change (Fig. 3A, inset). We tested three different stimulation frequencies (100, 200 and 333 Hz) and normalized the amplitudes of train EPSCs to the first EPSC ($EPSC_1$) (Fig. 3B). We did not find any significant difference between contralateral and ipsilateral endbulbs ($P > 0.05$, $n = 2$ to 3). This suggests that loading dye into the cochlea does not influence the functional properties of the endbulb.

Calcium imaging from the endbulb

To perform calcium imaging of AN fibers we recognized endbulbs by their characteristic morphology in Texas red fluorescence, as well as by being adjacent to a healthy BC in brightfield (Fig. 4Ai, ii), and measured changes in fluorescence upon stimulation. In the example in Fig. 4A, three baseline images were taken (single frame in Fig. 4Aiii). Then we stimulated the AN fiber with a 14-pulse train at 200 Hz, which caused fluorescence increases in restricted regions of the endbulb (Fig. 4Aiv). We quantified these fluorescence changes using the $\Delta F/F$ with respect to the averaged baseline image (Fig. 4Av). For the example in Fig. 4A, we integrated the $\Delta F/F$ in two regions of interest within the endbulb, as well as one unlabeled region (grey box, Fig. 4iii–v). The two endbulb regions showed large increases in fluorescence following stimulation, which then decayed over time, eventually going below the baseline fluorescence (Fig. 4Avi). This probably resulted from bleaching of non-specific labeling or intrinsic fluorescence, because a similar decrease was observed outside labeled endbulbs (grey box in Fig. 4Aiii–v, grey trace in vi). We corrected for this bleaching by subtracing the $\Delta F/F$ of the non-endbulb region, which led to a more stable measurement (Fig. 4Avii).

To demonstrate the utility of this technique, we tested whether $GABA_BR$ activation affects calcium influx in the endbulb. Previous work has indicated that $GABA_BR$ activation reduces the presynaptic probability of release at the endbulb (Chanda and Xu-Friedman, 2010a), probably as a result of a decrease in calcium influx (Bean, 1989). Application of the $GABA_BR$ agonist baclofen reduced the peak $\Delta F/F$. We then washed out baclofen and simultaneously applied the $GABA_BR$ antagonist CGP55845. This led to complete recovery of the $\Delta F/F$ (Fig. 4Avii). On average, the $\Delta F/F$ decreased to 48 ± 5% of control in baclofen and recovered to 97 ± 3% in CGP55845 (Fig. 4viii, $n = 5$ endbulbs).

To test if $GABA_BR$ activation had any effect on the resting calcium level of the endbulb, we compared baseline brightness just before drug application with just after, in areas that showed fluorescence changes during stimulation (Fig. 4B). There were no obvious changes in baseline fluorescence upon addition of $GABA_BR$ agonists or antagonists. We saw a very small decrease in the baseline fluorescence after application of baclofen as well as after CGP55845 (99%, Fig. 4Bi and ii, $n = 5$ endbulbs), suggesting both changes resulted from bleaching. Thus, we were unable to detect any changes in resting calcium.

Discussion

Here we described a method for doing calcium imaging from AN endbulbs. We demonstrate how this can be used to report calcium influx, and its modulation by $GABA_BR$ activation. These are the first measurements of calcium transients at the endbulb. Furthermore, this technique appears to preserve the normal plasticity characteristics of AN fibers. This approach could be used to explore how synaptic activity as well as other neuromodulators influence calcium influx at the endbulb.

We find that usually only a restricted band of AN fibers is labeled by fluorescent dextrans. That is good for some applications. For calcium imaging, it is useful to study individual synapses in isolation, so that signals can be ascribed to the synapse of interest. However, for

NIH-PA Author Manuscript

NIH-PA Author Manuscript

NIH-PA Author Manuscript

anatomical studies, it may be useful to label the auditory nerve more completely. For that, other dyes may be useful, such as diI (Maruyama and Ohmori, 2006) or neurobiotin (Limb and Ryugo, 2000). A related issue is that endbulbs tend to be reliably identifiable and functional when a postsynaptic BC is present. However, during slice preparation in mature AVCN, the number of surviving cells can be quite small, so labeling a larger band of fibers would allow greater chance of finding a healthy endbulb. For the purposes of this paper, we resolved that issue by studying animals just after the onset of hearing, when BC survival is better.

This technique could be improved in a number of ways over what is presented here. One issue is to increase the sensitivity. It would be desirable to measure responses to single stimuli, but these were difficult to discern by eye. To resolve this, we used long trains of activity that presumably produce large calcium rises, which required only 2 or 3 repetitions to produce large signals. Furthermore, improving the sensitivity would allow using dyes with lower affinity. Low-affinity dyes are ideal because they reflect calcium concentration in a linear manner, and provide a more faithful representation of the time-course of residual calcium in the presynaptic terminal. The major drawback of low-affinity dyes is their lower sensitivity to low concentrations of calcium. The high-affinity dyes we used here are non-linear but more sensitive. This may be resolved using a more sensitive detector, such as a photomultiplier tube. Photomultiplier tubes do not allow image formation, but that is not a problem for this application because calcium rises are only seen in very limited areas of the endbulb, and not, for example, in the axon shaft. Thus it is not necessary to screen out inappropriate signals based on their spatial location.

This technique will fill an important gap in the direct assessment of endbulb activity. Whole-cell patch techniques have anecdotally been brought to bear on the endbulb, which will open up a better understanding of its electrical properties. However, whole-cell patching does have drawbacks. One is that intracellular signaling pathways may be disrupted by the artificial internal solution. Calcium dyes do not greatly disrupt signaling if they are applied at low concentration. Additional calibration approaches would be needed to measure the exact dye concentration this method yields. Furthermore, calcium imaging allows measurement of terminal resting calcium levels, which drive a number of processes that are observed at the endbulb, including delayed release (Yang and Xu-Friedman, 2010) and activity-dependent recovery from depression (Yang and Xu-Friedman, 2008). In addition, other calcium-dependent processes have been implicated in synaptic plasticity, such as calcium-dependent calcium-channel inactivation or facilitation (Lee et al., 1999; Few et al., 2005; Xu and Wu, 2005; Mochida et al., 2008) and extracellular calcium depletion (Borst and Sakmann, 1999; Egelman and Montague, 1999). This technique could be used to evaluate these processes at the endbulb. In addition, labeling AN fibers also led to labeling of terminals in the DCN. While we did not examine calcium transients in the DCN here, that may prove useful to physiologists studying those areas.

Research highlights

- Dextran-conjugated fluorophores were injected into the cochlea.
- Calcium transients in the auditory nerve terminals were measured from the changes in fluorescence upon stimulation.
- Calcium transients were modulated by presynaptic $GABA_B$ receptor activation.

NIH-PA Author Manuscript

NIH-PA Author Manuscript

NIH-PA Author Manuscript

Acknowledgments

This study was supported by National Institutes of Health grant R01 DC 008125 to MAX-F. We particularly thank D. Ryugo for his advice and suggestions on the surgical method, and K. Mackie for the generous gift of the CB1R antibody. We also thank W. Sigurdson for assistance acquiring some images. Finally, we thank L. Pliss, J. Trimper and H. Yang for their help during the project and for comments on the manuscript.

References

Bean BP. Neurotransmitter inhibition of neuronal calcium currents by changes in channel voltage dependence. Nature. 1989; 340:153–156. [PubMed: 2567963]

Bellingham MC, Lim R, Walmsley B. Developmental changes in EPSC quantal size and quantal content at a central glutamatergic synapse in rat. J Physiol. 1998; 511(Pt 3):861–869. [PubMed: 9714866]

Borst JG, Sakmann B. Depletion of calcium in the synaptic cleft of a calyx-type synapse in the rat brainstem. J Physiol. 1999; 521(Pt 1):123–133. [PubMed: 10562339]

Brawer JR, Morest DK. Relations between auditory nerve endings and cell types in the cat's anteroventral cochlear nucleus seen with the Golgi method and Nomarski optics. J Comp Neurol. 1975; 160:491–506. [PubMed: 1091667]

Cant NB, Casseday JH. Projections from the anteroventral cochlear nucleus to the lateral and medial superior olivary nuclei. J Comp Neurol. 1986; 247:457–476. [PubMed: 3722446]

Chanda S, Xu-Friedman MA. Neuromodulation by GABA Converts a Relay into a Coincidence Detector. J Neurophysiol. 2010a

Chanda S, Xu-Friedman MA. A Low-affinity Antagonist Reveals Saturation and Desensitization in Mature Synapses in the Auditory Brainstem. J Neurophysiol. 2010b; 103:1915–1926. [PubMed: 20107122]

Egelman DM, Montague PR. Calcium dynamics in the extracellular space of mammalian neural tissue. Biophys J. 1999; 76:1856–1867. [PubMed: 10096884]

Fekete DM, Rouiller EM, Liberman MC, Ryugo DK. The central projections of intracellularly labeled auditory nerve fibers in cats. J Comp Neurol. 1984; 229:432–450. [PubMed: 6209306]

Few AP, Lautermilch NJ, Westenbroek RE, Scheuer T, Catterall WA. Differential regulation of CaV2.1 channels by calcium-binding protein 1 and visinin-like protein-2 requires N-terminal myristoylation. J Neurosci. 2005; 25:7071–7080. [PubMed: 16049184]

Gardner SM, Trussell LO, Oertel D. Time course and permeation of synaptic AMPA receptors in cochlear nuclear neurons correlate with input. J Neurosci. 1999; 19:8721–8729. [PubMed: 10516291]

Grynkiewicz G, Poenie M, Tsien RY. A new generation of Ca2+ indicators with greatly improved fluorescence properties. J Biol Chem. 1985; 260:3440–3450. [PubMed: 3838314]

Heinz MG, Young ED. Response growth with sound level in auditory-nerve fibers after noise-induced hearing loss. J Neurophysiol. 2004; 91:784–795. [PubMed: 14534289]

Lee A, Wong ST, Gallagher D, Li B, Storm DR, Scheuer T, Catterall WA. Ca2+/calmodulin binds to and modulates P/Q-type calcium channels. Nature. 1999; 399:155–159. [PubMed: 10335845]

Limb CJ, Ryugo DK. Development of primary axosomatic endings in the anteroventral cochlear nucleus of mice. J Assoc Res Otolaryngol. 2000; 1:103–119. [PubMed: 11545139]

Lorente de Nó, R. The Primary Acoustic Nuclei. Raven Press; New York: 1981. p. 176

Maruyama A, Ohmori H. Fluorescent labeling of rat auditory brainstem circuits for synaptic and electrophysiological studies. J Neurosci Methods. 2006; 152:163–172. [PubMed: 16246426]

Mochida S, Few AP, Scheuer T, Catterall WA. Regulation of presynaptic Ca(V)2.1 channels by Ca2+ sensor proteins mediates short-term synaptic plasticity. Neuron. 2008; 57:210–216. [PubMed: 18215619]

Oertel D. The role of intrinsic neuronal properties in the encoding of auditory information in the cochlear nuclei. Curr Opin Neurobiol. 1991; 1:221–228. [PubMed: 1821185]

Oleskevich S, Walmsley B. Synaptic transmission in the auditory brainstem of normal and congenitally deaf mice. J Physiol. 2002; 540:447–455. [PubMed: 11956335]

NIH-PA Author Manuscript

NIH-PA Author Manuscript

NIH-PA Author Manuscript

Ostapoff EM, Morest DK. Synaptic organization of globular bushy cells in the ventral cochlear nucleus of the cat: a quantitative study. J Comp Neurol. 1991; 314:598–613. [PubMed: 1814977]

Regehr WG, Tank DW. Selective fura-2 loading of presynaptic terminals and nerve cell processes by local perfusion in mammalian brain slice. J Neurosci Methods. 1991; 37:111–119. [PubMed: 1881195]

Ryugo DK, Fekete DM. Morphology of primary axosomatic endings in the anteroventral cochlear nucleus of the cat: a study of the endbulbs of Held. J Comp Neurol. 1982; 210:239–257. [PubMed: 7142440]

Ryugo DK, Sento S. Synaptic connections of the auditory nerve in cats: relationship between endbulbs of held and spherical bushy cells. J Comp Neurol. 1991; 305:35–48. [PubMed: 2033123]

Ryugo DK, Dodds LW, Benson TE, Kiang NY. Unmyelinated axons of the auditory nerve in cats. J Comp Neurol. 1991; 308:209–223. [PubMed: 1716268]

Saada AA, Niparko JK, Ryugo DK. Morphological changes in the cochlear nucleus of congenitally deaf white cats. Brain Res. 1996; 736:315–328. [PubMed: 8930338]

Salvi RJ, Henderson D, Hamernik R, Ahroon WA. Neural correlates of sensorineural hearing loss. Ear Hear. 1983; 4:115–129. [PubMed: 6345246]

Smith PH, Joris PX, Yin TC. Projections of physiologically characterized spherical bushy cell axons from the cochlear nucleus of the cat: evidence for delay lines to the medial superior olive. J Comp Neurol. 1993; 331:245–260. [PubMed: 8509501]

Smith PH, Joris PX, Carney LH, Yin TC. Projections of physiologically characterized globular bushy cell axons from the cochlear nucleus of the cat. J Comp Neurol. 1991; 304:387–407. [PubMed: 2022755]

Spirou GA, Brownell WE, Zidanic M. Recordings from cat trapezoid body and HRP labeling of globular bushy cell axons. J Neurophysiol. 1990; 63:1169–1190. [PubMed: 2358868]

Tsien RY. A non-disruptive technique for loading calcium buffers and indicators into cells. Nature. 1981; 290:527–528. [PubMed: 7219539]

Tucci DL, Rubel EW. Afferent influences on brain stem auditory nuclei of the chicken: effects of conductive and sensorineural hearing loss on n. magnocellularis. J Comp Neurol. 1985; 238:371–381. [PubMed: 4044922]

Wang Y, Manis PB. Short-term synaptic depression and recovery at the mature mammalian endbulb of Held synapse in mice. J Neurophysiol. 2008; 100:1255–1264. [PubMed: 18632895]

Xu J, Wu LG. The decrease in the presynaptic calcium current is a major cause of short-term depression at a calyx-type synapse. Neuron. 2005; 46:633–645. [PubMed: 15944131]

Yang H, Xu-Friedman MA. Relative roles of different mechanisms of depression at the mouse endbulb of Held. J Neurophysiol. 2008; 99:2510–2521. [PubMed: 18367696]

Yang H, Xu-Friedman MA. Developmental mechanisms for suppressing the effects of delayed release at the endbulb of Held. J Neurosci. 2010; 30:11466–11475. [PubMed: 20739568]

Zucker RS, Regehr WG. Short-term synaptic plasticity. Annu Rev Physiol. 2002; 64:355–405. [PubMed: 11826273]

NIH-PA Author Manuscript

NIH-PA Author Manuscript

NIH-PA Author Manuscript

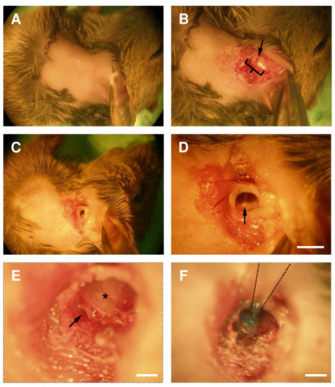

Figure 1.

Demonstration of the surgical approach in a euthanized animal. The animals lies on its right side, facing to the right, with its ventral side to the top of the field of view.

A. Hair from a small patch of postauricular skin was removed.

B. Incision was made in the postauricular area. Soft tissue was retracted to reveal the ear canal (bracket) and an incision was made in the clear area in the middle of the ear canal (arrow).

C. A small cut was made in the ear canal.

D. View of the tympanic membrane and the malleus (arrow). Scale bar = 1 mm.

E. Exposed view of round window (arrow) after removing part of the bulla. Asterisk – band shows the division point between the two turns of the cochlea. A hole is made in the cochlear wall just ventral to this. Scale bar = 0.1 mm.

F. A micropipette containing dye (Fast Green) was inserted into a hole drilled in the cochlea wall and the dye was pressure-injected. Scale bar = 0.2 mm.

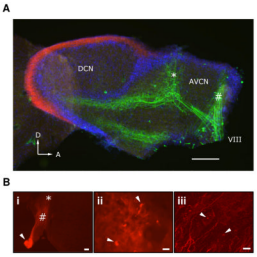

Figure 2.
AN labeling.
A. AN fibers were labeled by injection of dextran-conjugated fluorescein into the cochlea (green). In a sagittal section, the DCN molecular layer was counter-stained using CB1R immunohistochemistry with a Texas red-conjugated secondary antibody (red). Cell nuclei throughout the slice were counterstained using DAPI (blue). Scale bar = 200 μm. Arrowheads, D = Dorsal, A = Anterior. It appears that two distinct frequency bands of AN fibers were labeled, at low ("#") and high ("*") frequency.
B. AN fiber labeling using dextran-conjugated Texas red in a coronal section of cochlear nucleus. The AN root (arrow), AVCN (#) and DCN (*) are indicated (i). Scale bar = 100 μm. View of candidate endbulb terminals (ii, arrows). Scale bar = 10 μm. Putative synaptic terminals (iii, arrows) in the deep layers of the DCN. Scale bar = 10 μm.

NIH-PA Author Manuscript NIH-PA Author Manuscript NIH-PA Author Manuscript

NIH-PA Author Manuscript
NIH-PA Author Manuscript
NIH-PA Author Manuscript

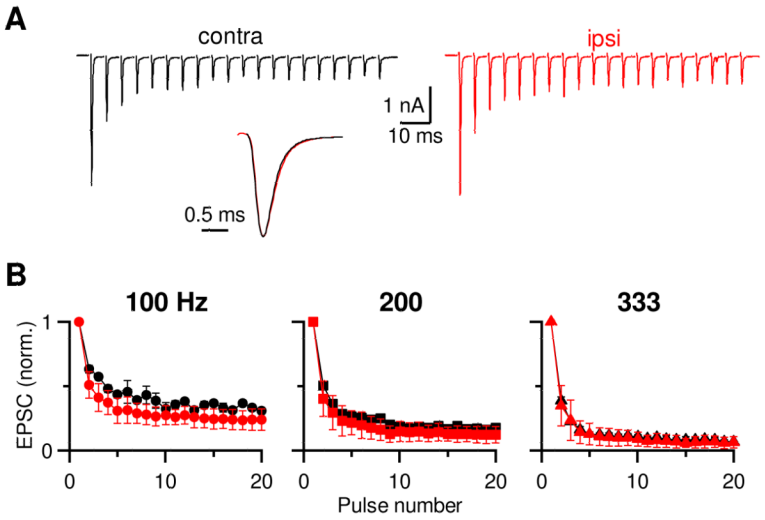

Fig 3.

Dye loading does not affect AN function.

A. Voltage-clamp recording from two BCs in AVCNs either contralateral (*left*) or ipsilateral (*right*) to the cochlea injected with dye. The AN inputs were stimulated with a 200-Hz train of 20 pulses. *Inset*: $EPSC_1$ from the two endbulbs scaled to the same amplitude.

B. Average normalized EPSC amplitude from 100, 200 and 333 Hz from dye-injected (red) and uninjected side (black).

NIH-PA Author Manuscript
NIH-PA Author Manuscript
NIH-PA Author Manuscript

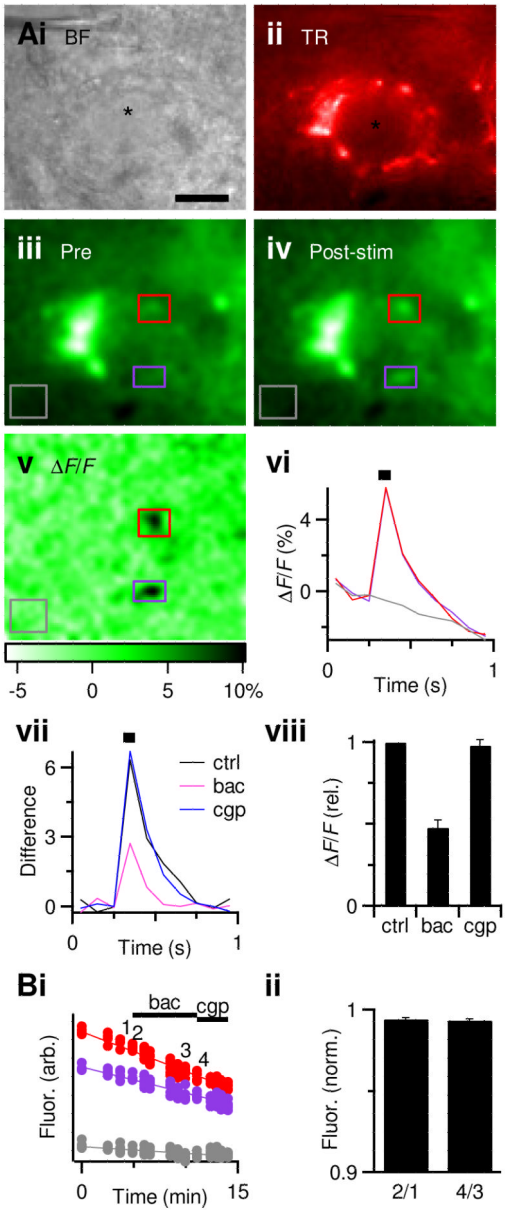

Figure 4.

$GABA_BR$ activation reduces presynaptic calcium influx.

A. Representative experiment showing BC (i) and endbulb, labeled by co-injection of dextran-conjugated Texas red (ii) and Oregon green (iii). Regions of interest are indicated by the purple and red boxes. The grey box represents an unlabeled region of interest to control for bleaching.

iv, Single frame showing fluorescence after endbulb stimulation (14 pulses at 200 Hz).

v, Changes in brightness, quantified as $\Delta F/F$, using the average of three pre-stimulus frames for the baseline fluorescence.

vi, Changes in $\Delta F/F$ following stimulation (black bar). Trace colors match the regions of interest indicated by the boxes in iii–v. The $\Delta F/F$ in the unlabeled region (grey trace) was used to correct for bleaching in the labeled regions (colored traces) by subtracting.

vii, Average corrected responses. Traces are averages of 2, 3, and 2 trials for control, baclofen, and CGP55845 respectively.

NIH-PA Author Manuscript

NIH-PA Author Manuscript

NIH-PA Author Manuscript

viii. Average effects of $GABA_BR$ activation on the corrected $\Delta F/F$ ($n = 5$). Baclofen significantly decreased the $\Delta F/F$ ($P < 0.001$, *t*-test), while CGP55845 was not significantly different from control conditions ($P > 0.2$).

B. Baseline fluorescence over the course of the experiment showing a steady decline as a result of bleaching (i), but no measurable changes resulting from drug application. ii, Average effects of $GABA_BR$ activation on baseline fluorescence levels. To enhance detection of possible decreases in resting calcium, without contamination by bleaching, the fluorescence just before drug application was compared to just after drug application (the timing of measurements “1” through “4” are indicated on the example experiment in i. The change into baclofen (“2/1”) was not significantly different from the change into CGP55845 (“4/3”), indicating no detectable change in resting calcium.